JOURNAL OF AIRCRAFT
Vol. 43, No. 6, November–December 2006

Efficient Computation of Robust Flutter Boundaries Using the μ–k Method

Dan Borglund* and Ulf Ringertz†
Royal Institute of Technology, 100 44 Stockholm, Sweden

DOI: 10.2514/1.20190

A simple and efficient algorithm for robust flutter analysis is presented. First, a general linear fractional transformation formulation of the μ–k method is provided, making it straightforward to pose the uncertain flutter equation in a form suitable for structured singular value analysis. The new formulation establishes a close connection between μ–k flutter analysis and traditional frequency-domain flutter analysis, which is used to formulate an efficient algorithm for computation of robust flutter boundaries. The proposed method is successfully applied to an F-16 sample test case with uncertain external stores aerodynamics, showing that standard tools for structural dynamics and unsteady aerodynamics can be used to perform robust flutter analysis with only modest additional modeling.

Introduction

ROBUST flutter analysis deals with aeroelastic (or aeroservoelastic) stability analysis taking model uncertainty into account. The overall aim of this research is to obtain a more reliable prediction of aeroelastic instabilities, both in analysis and flight testing, as these can be very sensitive even to small variations in parameters, loads, and boundary conditions. An overview of the numerous sources of uncertainty in aeroelasticity is provided in a recent review paper by Petit [1], where it is concluded that aerodynamic model uncertainty is often a greater concern than uncertainty i n the structural model. Petit also identifies two conceptually different approaches to robust flutter analysis; probabilistic analysis resulting in a probability distribution of the flutter boundary, and deterministic analysis resulting in an estimated worst-case flutter boundary.

This work is a contribution to the latter approach mentioned above, where a norm-bounded deterministic uncertainty is considered. A promising path in this area of research was initiated by Lind and Brenner [2,3] who demonstrated the use of so-called μ-analysis from the control community to perform robust flutter analysis. In a successive effort, Borglund [4] combined classical frequency-domain aeroelasticity with μ-analysis to formulate the μ–k method, being closely related to the p–k and g-methods [5,6]. Means to model aerodynamic uncertainty and to compute an upper bound on the flutter speed have also been provided [4,7].

In this paper, a more general linear fractional transformation (LFT) formulation of the μ–k method is introduced, and a simple μ–k algorithm that exploits the results from a standard p–k or g-method flutter analysis is outlined. The problem of developing a minimum-size aerodynamic uncertainty description is also treated in more detail than in previous work [4]. Finally, the proposed procedure is applied to an F-16 sample test case, showing how standard analysis tools such as NASTRAN [8] and ZAERO [9] can be used to develop uncertainty descriptions and perform robust flutter analysis.

Presented at the EADS/CEAS/DLR/AIAA International Forum on Aeroelasticity and Structural Dynamics 2005, Munich, 28 June–1 July 2005; received 22 September 2005; revision received 20 March 2006; accepted for publication 6 April 2006.

*Research Associate, Department of Aeronautical and Vehicle Engineering, Division of Flight Dynamics, Teknikringen 8. Member AIAA.

†Professor, Department of Aeronautical and Vehicle Engineering, Division of Flight Dynamics, Teknikringen 8. Member AIAA.

μ–k Method

In the Laplace-domain, the aeroelastic equations of motion of an airframe can be written in the nondimensional form

$$\boldsymbol{F}_0(p)\boldsymbol{\eta} = [\boldsymbol{M}_0 p^2 + (L^2/V^2)\boldsymbol{K}_0 - (\rho L^2/2)\boldsymbol{Q}_0(p, M)]\boldsymbol{\eta} = \boldsymbol{0} \quad (1)$$

where $\boldsymbol{M}_0$ is the mass matrix, $\boldsymbol{K}_0$ is the stiffness matrix, $\boldsymbol{Q}_0(p, M)$ is the aerodynamic transfer matrix and $\boldsymbol{\eta}$ is the vector of modal coordinates. All matrices are n_m by n_m, where n_m is the number of modes used in the modal basis. Further, V is the airspeed, L is the aerodynamic reference length, ρ is the air density and M is the Mach number. The nondimensional Laplace variable is denoted $p = g + ik$, where g is the damping and k is the reduced frequency.

The flutter Eq. (1) is a nonlinear eigenvalue problem that defines a set of eigenvalues p and eigenvectors $\boldsymbol{\eta}$. With the p–k or g-methods [5,6], this eigenvalue problem is solved in an approximate fashion to detect when an eigenvalue crosses the stability boundary $g = 0$. At this flight condition there is a critical flutter eigenvalue $p = ik$ making $\boldsymbol{F}_0(ik)$ singular, where the corresponding value of k is the reduced flutter frequency. Flutter analysis in the absence of model uncertainty will be referred to as nominal flutter analysis in the following.

LFT Formulation

The μ–k method extends the standard formulation to take deterministic model uncertainty into account. The flutter Eq. (1) is modified to include uncertain parameters (or dynamics [7]) and posed in the LFT form

$$\mathcal{F}_u[\boldsymbol{N}(p), \Delta]\boldsymbol{\eta} = [\boldsymbol{N}_{22} + \boldsymbol{N}_{21}\Delta(\boldsymbol{I} - \boldsymbol{N}_{11}\Delta)^{-1}\boldsymbol{N}_{12}]\boldsymbol{\eta} = 0 \quad (2)$$

where the upper LFT $\mathcal{F}_u(\boldsymbol{N}, \Delta)$ represents the uncertain transfer matrix between the modal coordinates $\boldsymbol{\eta}$ and force $\boldsymbol{\xi}$ shown in Fig. 1a. The transfer matrix $\boldsymbol{N}(p)$ depends on the flight condition and is partitioned with respect to the input and output signals according to

$$\boldsymbol{N}(p) = \begin{bmatrix} \boldsymbol{N}_{11} & \boldsymbol{N}_{12} \\ \boldsymbol{N}_{21} & \boldsymbol{N}_{22} \end{bmatrix} \quad (3)$$

where $\boldsymbol{N}_{22}(p)$ is n_m by n_m and the sizes of the remaining partitions depend on the uncertainty description. The uncertainty parameters are isolated to the block-structured matrix Δ and are usually scaled such that Δ belongs to a set $\mathcal{S}_\Delta$ defined as

$$\mathcal{S}_\Delta = \{\Delta : \Delta \in \boldsymbol{\Delta} \quad \text{and} \quad \bar{\sigma}(\Delta) \leq 1\} \quad (4)$$

where the set $\boldsymbol{\Delta}$ defines the block structure and $\bar{\sigma}(\cdot)$ denotes the maximum singular value. In cases where the uncertainty parameters

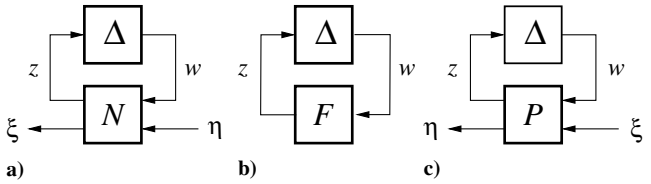

Fig. 1 a) LFT between η and ξ, b) feedback loop, and c) LFT between ξ and η.

are defined such that $\Delta = 0$ represents the nominal model, $\boldsymbol{N}_{22}(p) = \boldsymbol{F}_0(p)$ and the close connection between Eqs. (1) and (2) is apparent.

By considering the LFT in Fig. 1a with $\boldsymbol{\xi} = 0$, it is clear that Eq. (2) is a reduced form of the feedback equations

$$\boldsymbol{w} = \Delta \boldsymbol{z} \tag{5}$$

$$\boldsymbol{z} = \boldsymbol{N}_{11}\boldsymbol{w} + \boldsymbol{N}_{12}\boldsymbol{\eta} \tag{6}$$

$$\boldsymbol{0} = \boldsymbol{N}_{21}\boldsymbol{w} + \boldsymbol{N}_{22}\boldsymbol{\eta} \tag{7}$$

If it is assumed that $\boldsymbol{N}_{22}(p)$ is nonsingular, these equations can also be reduced to the feedback form

$$[\boldsymbol{I} - \boldsymbol{F}(p)\Delta]\boldsymbol{z} = 0 \tag{8}$$

where the system matrix

$$\boldsymbol{F}(p) = \boldsymbol{N}_{11} - \boldsymbol{N}_{12}\boldsymbol{N}_{22}^{-1}\boldsymbol{N}_{21} \tag{9}$$

is completely determined by the LFT transfer matrix $\boldsymbol{N}(p)$. Note that Eq. (8) is the governing equation of the feedback system in Fig. 1b. The problem of posing the uncertain flutter equation in the feedback form Eq. (8), which is central to the μ–k method, is now a matter of finding a LFT representation $\mathcal{F}_u(\boldsymbol{N}, \Delta)$.

Example

Consider the case when the aeroelastic equations of motion depend linearly on a set δ_j of uncertainty parameters and a fixed (nominal) modal basis is used. Let the real-valued parameters (typically representing perturbations to the mass and stiffness distributions) be scaled such that $\delta_j \in [-1, 1]$ and the complex-valued parameters (typically representing perturbations to the frequency-domain aerodynamic forces) be scaled such that $|\delta_j| \leq 1$. The uncertain flutter equation can then be written in the form

$$[\boldsymbol{F}_0(p) + \boldsymbol{F}_L(p)\Delta\boldsymbol{F}_R(p)]\boldsymbol{\eta} = 0 \tag{10}$$

where the uncertainty matrix Δ is diagonal with multiples of the uncertainty parameters δ_j on the diagonal (defining the block-diagonal structure) and satisfies the norm-bound $\bar{\sigma}(\Delta) \leq 1$. The number of modes used in the modal basis bounds the size of each block, such that each parameter is repeated up to n_m times [4]. $\boldsymbol{F}_0(p)$ is commonly the nominal transfer matrix defined in Eq. (1), and $\boldsymbol{F}_L(p)$ and $\boldsymbol{F}_R(p)$ are scaling matrices that determine the magnitude of the uncertainty and how the uncertainty parameters influence the dynamics.

In this case, it is trivial to identify the LFT transfer matrix

$$\boldsymbol{N}(p) = \begin{bmatrix} \boldsymbol{N}_{11} & \boldsymbol{N}_{12} \\ \boldsymbol{N}_{21} & \boldsymbol{N}_{22} \end{bmatrix} = \begin{bmatrix} 0 & \boldsymbol{F}_R \\ \boldsymbol{F}_L & \boldsymbol{F}_0 \end{bmatrix} \tag{11}$$

by comparing Eqs. (2) and (10). This gives the system matrix

$$\boldsymbol{F}(p) = -\boldsymbol{F}_R\boldsymbol{F}_0^{-1}\boldsymbol{F}_L \tag{12}$$

that is well-defined except at the nominal eigenvalues where $\boldsymbol{N}_{22}(p) = \boldsymbol{F}_0(p)$ is singular. In a more difficult case, perhaps involving higher-order parametric perturbations, it is possible to define individual LFTs for the different terms in the flutter equation and then use straightforward LFT operations [10] to assemble $\mathcal{F}_u(\boldsymbol{N}, \Delta)$. □

It is also useful to consider the inverse LFT from the input $\boldsymbol{\xi}$ to the output $\boldsymbol{\eta}$ in Fig. 1c. By application of the LFT inverse theorem [10] this LFT is $\mathcal{F}_u(\boldsymbol{P}, \Delta)$, where

$$\boldsymbol{P}(p) = \begin{bmatrix} \boldsymbol{P}_{11} & \boldsymbol{P}_{12} \\ \boldsymbol{P}_{21} & \boldsymbol{P}_{22} \end{bmatrix} = \begin{bmatrix} \boldsymbol{N}_{11} - \boldsymbol{N}_{12}\boldsymbol{N}_{22}^{-1}\boldsymbol{N}_{21} & -\boldsymbol{N}_{12}\boldsymbol{N}_{22}^{-1} \\ \boldsymbol{N}_{22}^{-1}\boldsymbol{N}_{21} & \boldsymbol{N}_{22}^{-1} \end{bmatrix} \tag{13}$$

This provides the alternative definition

$$\boldsymbol{F}(p) = \boldsymbol{P}_{11} \tag{14}$$

of the system matrix (as given in [4]). However, the definition Eq. (9) is more useful because finding a representation $\mathcal{F}_u(\boldsymbol{N}, \Delta)$ is simply a matter of reformulating the uncertain flutter equation. But Eq. (13) is still an important result for model validation purposes, where $\mathcal{F}_u(\boldsymbol{P}, \Delta)$ can be used for prediction of input–output frequency responses of the uncertain system [4,11,12].

Robust Flutter Analysis

The flutter Eq. (2) is an uncertain nonlinear eigenvalue problem that for each $\Delta \in \mathcal{S}_\Delta$ defines a set of eigenvalues p and eigenvectors $\boldsymbol{\eta}$. Robust flutter analysis is about finding the flight conditions where some $\Delta \in \mathcal{S}_\Delta$ enables a critical eigenvalue $p = ik$. With the μ–k method, this is accomplished by direct application of structured singular value analysis to the feedback form Eq. (8) of the uncertain flutter equation.

The structured singular value μ of the system matrix $\boldsymbol{F}(ik)$ is defined as the reciprocal of the minimum norm of any matrix $\Delta \in \boldsymbol{\Delta}$ making $[\boldsymbol{I} - \boldsymbol{F}(ik)\Delta]$ singular, giving

$$\mu[\boldsymbol{F}(ik)] = 1/\min_{\Delta\in\Delta}\{\bar{\sigma}(\Delta): \det[\boldsymbol{I} - \boldsymbol{F}(ik)\Delta] = 0\} \tag{15}$$

By definition, $\mu[\boldsymbol{F}(ik)] = 0$ if no $\Delta \in \boldsymbol{\Delta}$ makes $[\boldsymbol{I} - \boldsymbol{F}(ik)\Delta]$ singular. This means that no eigenvalue $p = ik$ is possible for $\Delta \in \mathcal{S}_\Delta$ if

$$\mu(k) = \mu[\boldsymbol{F}(ik)] < 1 \tag{16}$$

holds for all frequencies $k > 0$. Then a nominally stable flight condition is also robustly stable (stable in the presence of uncertainty) and a nominally unstable flight condition is also robustly unstable [7]. The robust flutter boundaries are thus defined by the flight conditions where the peak value of $\mu(k)$ crosses the robust stability boundary $\mu = 1$.

Example

In the subsequent F-16 case study, the aerodynamic uncertainty descriptions leads to a flutter equation in the form Eq. (10). In the most simple cases there is only one complex-valued uncertainty parameter δ, leading to an uncertainty matrix $\Delta = \delta\boldsymbol{I}$. The parameter is bounded to the unit disc such that $|\delta| \leq 1$ and $\bar{\sigma}(\Delta) \leq 1$ hold. In such a simple case, robust stability can be investigated by performing a p–k flutter analysis for a discretized set of values of the uncertainty parameter. Assuming that the most critical perturbation will satisfy $|\delta| = 1$, it is sufficient to consider the values $\delta = e^{i\varphi}$ on the unit circle, where $\varphi \in (0, 2\pi)$.

To illustrate the close relationship between p–k and μ–k flutter analysis, both analyses were performed for one of the investigated uncertainty descriptions at Mach number $M = 0.8$. The particular model and uncertainty description is not of importance here, only that a relevant model is used and that the flutter equation depends on one complex-valued uncertainty parameter. For completeness, however, the particular uncertainty description will be referred to in the case study.

Figure 2 shows a root-locus graph of the critical p–k eigenvalue using the flight altitude h as continuation parameter. At altitude $h_5 = 5577$ m, the nominal eigenvalue is stable. Computing the p–k eigenvalues for a set of δ values on the unit circle, it is found that the perturbed eigenvalues are confined to an elliptic region in this case. Further, the elliptic region is oriented such that the damping of the flutter mode is more sensitive to the aerodynamic perturbation than

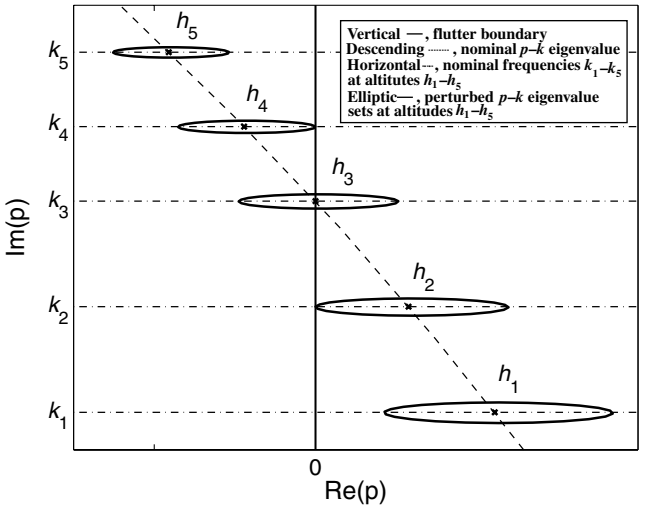

Fig. 2 Root-locus graph.

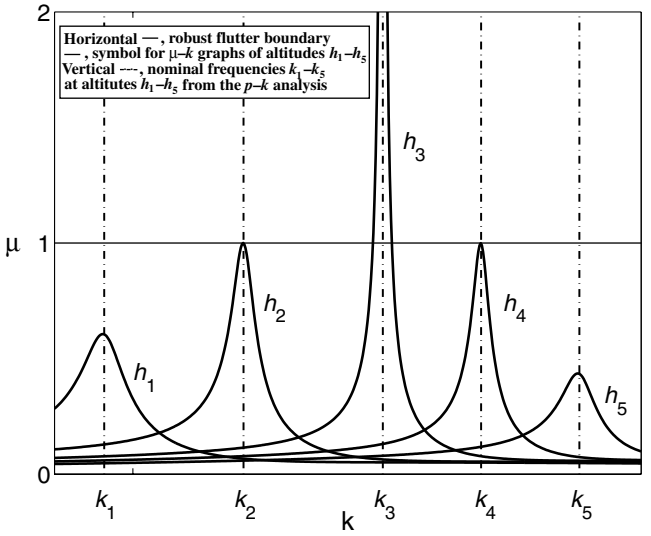

Fig. 3 μ–k graphs at altitudes h_1–h_5 from the p–k analysis.

the frequency. Because all perturbed eigenvalues are stable, this flight condition is robustly stable.

Reducing the altitude to $h_4 = 4907$ m, the corresponding elliptic region touches the imaginary axis in the root-locus graph. This means that some parameter δ in the unit disc (or some $\Delta \in \mathcal{S}_\Delta$) enables a critical eigenvalue $p = ik$, and h_4 is the worst-case flutter altitude. Below this altitude there is a potential risk for flutter.

The altitude $h_3 = 4237$ m is the nominal flutter boundary at which the nominal eigenvalue is located on the imaginary axis. At this altitude the elliptic region crosses the imaginary axis, and the flight condition is either stable or unstable. In this case, the uncertainty enables a range of critical eigenvalues $p = ik$ on the imaginary axis, defining the possible flutter frequencies.

The best-case flutter altitude is $h_2 = 3288$ m, below which all perturbed eigenvalues are unstable (illustrated for $h_1 = 2338$ m). The robust flutter analysis will thus divide the flight envelope into regions that are either 1) robustly stable, 2) stable or unstable, or 3) robustly unstable.

Using the μ–k method, each flight condition is represented by a μ–k graph. When the nominal eigenvalue approaches the stability boundary (from either side), the norm of the uncertainty required to destabilize (or stabilize) the system tends to zero. In the μ–k graph this will become visible as a distinct peak in the neighborhood of the frequency of the eigenvalue. In the case of one complex-valued uncertainty parameter δ, the function $\mu(k) = \rho[\boldsymbol{F}(ik)]$, where $\rho[\boldsymbol{F}(ik)]$ is the spectral radius of $\boldsymbol{F}(ik)$. This result is easily obtained from the definition Eq. (15) with $\Delta = \delta \boldsymbol{I}$. Because the spectral radius can be computed exactly, the peak of the μ–k graph should touch the robust stability boundary $\mu = 1$ at the altitudes h_2 and h_4, at the frequencies where the corresponding elliptic regions in Fig. 2 touch the imaginary axis.

The μ–k graphs for the altitudes h_1–h_5 are shown in Fig. 3. At altitude h_5, the graph satisfies $\mu(k) < 1$ and because this flight condition is nominally stable it is also robustly stable. As predicted, the peak of the μ–k graph touches the robust flutter boundary $\mu = 1$ at the worst-case flutter altitude h_4. At the nominal flutter altitude h_3, the μ–k graph displays a singularity at the nominal flutter frequency because no uncertainty is required to destabilize the system at this flight condition. Further, in the μ–k analysis, the possible flutter frequencies are defined by the frequency range where $\mu(k) \geq 1$. At the best-case flutter altitude h_2, the peak crosses the robust stability boundary again and at altitude h_1, the flight condition is robustly unstable (as predicted by the p–k analysis) because it is nominally unstable and $\mu(k) < 1$. Note that the μ–k graph in itself is not sufficient to determine if the flight condition is robustly stable or unstable (see, for example, the graphs for h_1 and h_5 in Fig. 3), but that nominal stability also has to be considered to decide on this.

While it becomes unrealistic to map the perturbed eigenvalues for a more general uncertainty description (involving a larger number of uncertainty parameters), the μ–k method can still be applied. The main difference, besides an increased computational cost, is that the robust stability criterion Eq. (16) has to be evaluated using computable upper bounds for μ [13].

Algorithm

The nominal frequencies k_1–k_5 shown in Fig. 2 are the imaginary parts of the p–k eigenvalues at the altitudes h_1–h_5. These frequencies also have been indicated in Fig. 3. Clearly, the nominal frequency is a quite good estimate of the location of the corresponding peak in the μ–k graph. The accuracy of this estimate is expected to increase the closer the nominal eigenvalue is to the stability boundary because the nominal and peak frequencies will coalesce at the nominal flutter boundary (visible in Fig. 3). These observations suggest that the following simple algorithm can be used for computation of the robust flutter boundaries:

For each mode and Mach number of interest:

1) First the nominal eigenvalue is computed for a discrete set of altitudes using the p–k or g-methods. From this data, the nominal frequency $k_{\text{nom}}(h)$ as function of altitude can be obtained by interpolation.

2) The corresponding peak value $\mu_{\text{peak}}(h)$ as function of altitude can now be computed by solving a univariate maximization problem using the frequency as variable and $k_{\text{nom}}(h)$ as initial guess for the peak frequency. In this study, golden-section search [14] was used for this purpose.

3) The peak value $\mu_{\text{peak}}(h)$ is computed for a discrete set of altitudes. By detecting when the peak value crosses $\mu = 1$, upper and lower bounds on the robust flutter altitudes are obtained.

4) Finally, bisection [14] is used to compute the robust flutter altitudes to within a given tolerance h_{tol}.

Note that the nominal data only has to be computed once, even if several uncertainty descriptions are to be investigated. Of course, this data can also be used for computation of the nominal flutter boundary.

The given μ–k algorithm has about the same complexity as a basic version of the p–k algorithm [5]. It is simple and robust, and no derivatives of μ are required. Another advantage is that the use of nominal data makes it possible to track modes, making it very efficient compared to an implementation based on a direct computation of high-resolution μ–k graphs. As long as the critical modes are tracked, the possibility of flutter modes switching with the uncertainty is still accounted for. The robust flutter speed is simply the lowest worst-case flutter speed of the different modes. In this aspect, there is no difference between μ–k analysis and standard frequency-domain flutter analysis. Basically, the μ–k method just extends the standard formulation to take model uncertainty into account.

F-16 Sample Test Case

To illustrate the computation of robust flutter boundaries using the μ–k method, the results obtained on a test case using a prototype algorithm will be presented. The test case is a reasonably accurate representation of the F-16 Falcon with an external stores configuration known as MA41. The external stores are two LAU-129 launchers, two MK-84 bombs, two 370 gal fuel tanks, one 300 gal central fuselage tank, and wing tip Sidewinder missiles. This configuration is known to experience aeroelastic instabilities for Mach numbers in the range 0.6–1.0 as described in [15].

The model is available as a test case in the ZAERO applications manual [16]. The structure is modeled in NASTRAN using a combination of beam and shell elements, and the lowest 15 antisymmetric modes are used to define the modal basis. The modes represent three rigid body modes and 12 elastic modes in the frequency range 5.4–18.3 Hz. The aerodynamic model, shown in Fig. 4, is fairly detailed in terms of modeling the wing and external stores but with a more schematic representation of the fuselage. A total of $n_b = 1016$ aerodynamic boxes are used to model one half of the aircraft as the geometry is assumed symmetrical.

In [15], it is concluded that the external stores aerodynamics has a significant impact on the flutter speed, and that the flutter speed appears to be sensitive to the aerodynamic modeling of the outboard underwing and tip launchers. Because of the difficulties with modeling external stores aerodynamics accurately, it is desirable to take aerodynamic uncertainty into account in the flutter analysis. As will be demonstrated in the following, this can be accomplished in a straightforward fashion with the μ–k method. Note that the objective here is not to deliver results for comparison with flight test data, but merely to demonstrate this capability for a realistic case with a realistic (but not validated) uncertainty description. The type of aerodynamic uncertainty description derived in [4] will be applied for this purpose, which is described in the following.

Uncertainty description

To define the aerodynamic uncertainty model, it is necessary to partition the aerodynamic matrix according to

$$\boldsymbol{Q}_0(ik, M) = \boldsymbol{L}\boldsymbol{R}(ik, M) \tag{17}$$

where the n_b by n_m matrix $\boldsymbol{R}(ik, M)$ defines the mapping from modal coordinates to lifting surface-pressure coefficients, and the n_m by n_b matrix $\boldsymbol{L}$ defines the mapping from lifting surface-pressure coefficients to generalized forces. Note that $\boldsymbol{L}$ is independent of the reduced frequency and the Mach number because it is made up of information from the spline interface between structural and aerodynamic models and modal eigenvector information.

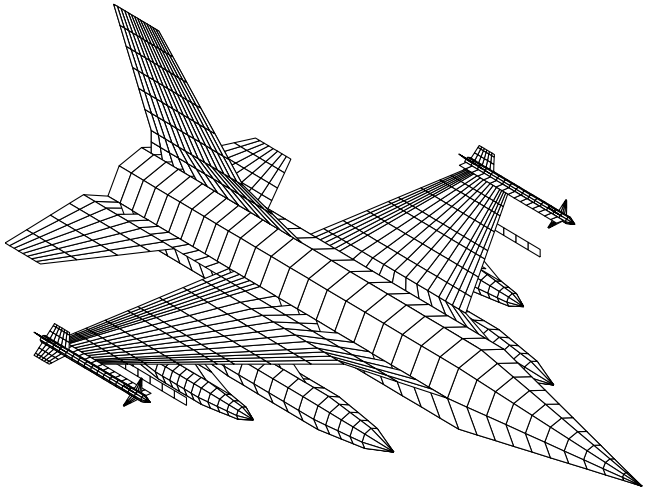

Fig. 4 ZAERO aerodynamic model of the F-16 MA41 configuration.

If the partitioned aerodynamic matrices are available, it is possible to define aerodynamic uncertainty descriptions by selecting the appropriate rows and columns of the partitioned matrices as described in the following. Fortunately, ZAERO stores most analysis information on a database file and tools for accessing information on this database file are provided [9]. In the present study, the required matrices and other information was extracted from the ZAERO database file and stored on a file, which was then read by a small MATLAB program that performed the actual robust flutter analysis.

As described in more detail in [4], the partitioned aerodynamic matrices in Eq. (17) can be used for modeling of uncertainty in the lifting surface-pressure coefficients of the nominal model. The boxes in the aerodynamic model are divided into different patches with associated multiplicative uncertainties. This leads to an uncertain aerodynamic matrix that can be written in the form

$$\boldsymbol{Q} = \boldsymbol{Q}_0 + \sum_{j=1}^{n_p} w_j \delta_j \boldsymbol{Q}_j = \boldsymbol{Q}_0 + \sum_{j=1}^{n_p} \boldsymbol{Q}_{Lj} \Delta_{Qj} \boldsymbol{Q}_{Rj} = \boldsymbol{Q}_0 + \boldsymbol{Q}_L \Delta_Q \boldsymbol{Q}_R \tag{18}$$

where n_p is the number of uncertain patches and the real weights $w_j \geq 0$ scales the aerodynamic perturbations such that the complex uncertainty parameters δ_j belongs to the set $|\delta_j| \leq 1$. The perturbation matrices $\boldsymbol{Q}_j = \boldsymbol{L}_j \boldsymbol{R}_j$, where $\boldsymbol{L}_j$ is the matrix composed of the rows of $\boldsymbol{L}$ corresponding to the boxes in patch j, and $\boldsymbol{R}_j$ is the matrix composed of the columns of $\boldsymbol{R}$ corresponding to the boxes in patch j. Consequently, a weight $w_j = 0.1$ means that a 10% uncertainty bound is assigned to the boxes in patch j, and that the corresponding pressure coefficients are perturbed in a uniform manner.

A minimum-size uncertainty matrix Δ_Q is obtained as follows. If the number of boxes n_j in patch j is smaller than the number of modes n_m used in the modal basis, then

$$\boldsymbol{Q}_{Lj} = \boldsymbol{L}_j \tag{19}$$

$$\Delta_{Qj} = \delta_j \boldsymbol{I}_{n_j \times n_j} \tag{20}$$

$$\boldsymbol{Q}_{Rj} = w_j \boldsymbol{R}_j \tag{21}$$

Otherwise,

$$\boldsymbol{Q}_{Lj} = \boldsymbol{Q}_j \tag{22}$$

$$\Delta_{Qj} = \delta_j \boldsymbol{I}_{n_m \times n_m} \tag{23}$$

$$\boldsymbol{Q}_{Rj} = w_j \boldsymbol{I}_{n_m \times n_m} \tag{24}$$

By this, the rank of the perturbation matrices $\boldsymbol{Q}_j$ will bound the size of each uncertainty block Δ_{Qj}. Finally, the total structure

$$\boldsymbol{Q}_L = \begin{bmatrix} \boldsymbol{Q}_{L1} & \boldsymbol{Q}_{L2} & \cdots & \boldsymbol{Q}_{Ln_p} \end{bmatrix} \tag{25}$$

$$\Delta_Q = \text{diag}(\Delta_{Q1}, \Delta_{Q2}, \ldots, \Delta_{Qn_p}) \tag{26}$$

$$\boldsymbol{Q}_R = \begin{bmatrix} \boldsymbol{Q}_{R1} & \boldsymbol{Q}_{R2} & \cdots & \boldsymbol{Q}_{Rn_p} \end{bmatrix}^T \tag{27}$$

of the aerodynamic uncertainty description is assembled.

If the aerodynamic matrix in the nominal flutter Eq. (1) is replaced with the uncertain aerodynamic matrix in Eq. (18), an uncertain flutter equation in the form Eq. (10) results, where

$$\boldsymbol{F}_L = -(\rho L^2/2)\boldsymbol{Q}_L \tag{28}$$

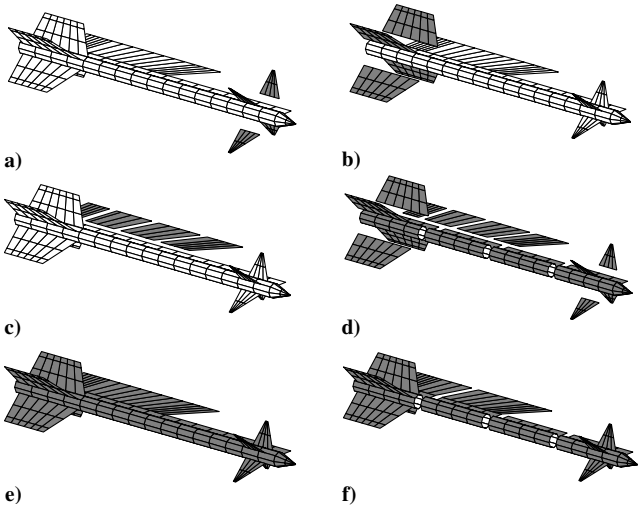

Fig. 5 Illustration of aerodynamic uncertainty descriptions. Uncertain patches are visualized as shaded sets of boxes.

$$\Delta = \Delta_Q \tag{29}$$

$$\boldsymbol{F}_R = \boldsymbol{Q}_R \tag{30}$$

From Eq. (12), this gives the frequency-domain system matrix

$$\boldsymbol{F}(ik) = (\rho L^2/2)\boldsymbol{Q}_R\boldsymbol{F}_0^{-1}\boldsymbol{Q}_L \tag{31}$$

in the case where only aerodynamic uncertainty is taken into account.

For the robust flutter analysis, the wing tip aerodynamic modeling is assumed to be the critical area of interest. This is confirmed by studying the flutter mode of the nominal flutter solution and also of the complex geometry of the wing tip with Sidewinder missile installed. Further, a simple modification such as removing the canard fins on the wing tip missile has a significant effect on the flutter altitude. The sensitivity of the flutter boundary will therefore be investigated by computing robust flutter boundaries for the six different uncertainty descriptions illustrated in Fig. 5. Only one patch is used in case a (missile canard fins), case b (missile tail fins), and case e (wing tip and stores), whereas several patches are used in case c (wing tip, four patches), case d (wing tip and stores, 10 patches), and case f (wing tip and stores, four patches). A 10% uncertainty bound is used for all patches in all cases.

Robust Flutter Boundaries

First, a MATLAB implementation of the modified p–k solver in [5] was used to compute the nominal flutter boundary in the altitude range 0–12 km and Mach number range 0.6–0.95. The solver was coupled with a model of the standard atmosphere to obtain match-point flutter solutions. A Mach number resolution $\Delta M = 0.01$ was used and a tolerance $h_{\text{tol}} = 10$ m was required for the flutter altitude. As shown in Fig. 6, the nominal ZAERO model predicts a flutter Mach number between 0.7 and 0.95 for altitudes 0–10 km. Further, the same flutter mode was predicted throughout the envelope, being dominated by the first antisymmetric wing bending and torsion structural modes.

As described in the preceding section, the μ–k algorithm was implemented in MATLAB, and the μ-toolbox [17] was used for the μ computations (using the default settings). Again, the solver was coupled with a model of the standard atmosphere to obtain match-point robust flutter solutions. The critical p–k eigenvalue was computed for a $\Delta h = 0.5$ km and $\Delta M = 0.01$ grid of the envelope and used for linear interpolation of the nominal frequency $k_{\text{nom}}(h)$ at the different Mach numbers. For each uncertainty description, the peak value $\mu_{\text{peak}}(h)$ was then computed for a more sparse set of altitudes. In this case, $\Delta h = 4$ km was used, but the nominal flutter altitude was added to this data to ensure at least one point in between

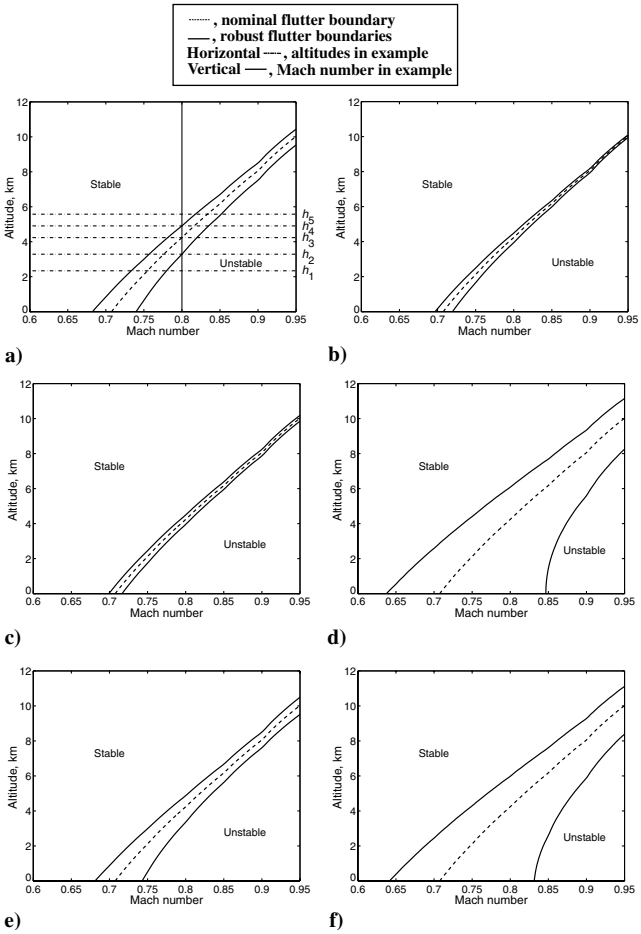

Fig. 6 Flutter boundaries for the different uncertainty descriptions.

the robust flutter altitudes. This step provided upper and lower bounds for the robust flutter altitudes at each Mach number. Finally, a Mach number sweep was performed, where bisection was used to compute the robust flutter altitudes to within a tolerance of $h_{\text{tol}} = 10$ m.

In this study, it was straightforward to solve the problems with the described μ–k solver, and the different robust flutter boundaries are shown in Fig. 6. In all cases, the flutter speed is the most sensitive to the aerodynamic uncertainty at low altitude (or at high speed). In case a (missile canard fins), the maximum perturbation of the flutter speed is about $-4\%/+5\%$ at zero altitude. This was also the case that was used in the previous example illustrating the connection between p–k and μ–k analysis, and the altitudes h_1–h_5 are indicated along with the corresponding Mach number $M = 0.8$. The nominal and robust flutter altitudes are readily verified.

The flutter boundary is found to be less sensitive to uncertainty in the missile tail fin aerodynamics (case b), showing a $-2\%/+2\%$ maximum perturbation of the flutter speed. Case c (wing tip) is the least sensitive with a $-1\%/+1\%$ maximum perturbation, while case d (wing tip and stores) is the most sensitive with a $-10\%/+20\%$ maximum perturbation. The reason for the asymmetry of the robust flutter boundaries is that the damping of the system is more sensitive to the uncertainty at higher speeds (visible in Fig. 2). According to the robust analysis, a 10% uncertainty in the wing tip aerodynamic modeling can thus reduce the predicted flutter speed by 10% in the worst case.

As expected, case d (wing tip and stores) has the largest influence on the flutter boundary. Case e is a simplified version of case d where only one patch is used. Somewhat surprisingly, this perturbation has about the same influence ($-4\%/+5\%$) as the canard fins only (case a). This means that the distribution of the aerodynamic perturbation has a significant influence in this case. This is because the flutter speed is very sensitive to the wing tip twist moment, which

Table 1 Properties of the uncertainty descriptions and results from robust flutter analysis at $M = 0.85$

Case	Description	n_p	Δ_Q	n_μ	t_c, S
a	missile canard fins	1	15×15	100	5
b	missile tail fins	1	15×15	84	4
c	wing tip	4	18×18	65	4
d	wing tip and stores	10	108×108	134	232
e	wing tip and stores	1	15×15	121	6
f	wing tip and stores	4	60×60	114	41

is confirmed by investigating case f. This case is limited to chordwise perturbations only, but the influence on the flutter boundary is very close to case d ($-9\%/+18\%$). If validated in flight testing, the difference between cases d and f would most likely be negligible. However, as will be shown in the next section, case f is preferable from a computational point of view.

Computational Aspects

The computational effort using μ-analysis depends strongly on the structure and size of the uncertainty description [13]. In Table 1, some results from robust flutter analysis at $M = 0.85$ for the different cases in Fig. 5 are presented, including the number of patches n_p, the size of the uncertainty matrix Δ_Q, the required number of μ evaluations n_μ, and the computational time t_c on an IBM T23 ThinkPad laptop.

For example, case a in Fig. 5 is defined by one uncertain patch only ($n_p = 1$), including all canard fins of the missile. Because the number of aerodynamic boxes in this patch (32) is greater than the number of modes used in the analysis (15), the minimum size of Δ_Q is 15×15. In this case, the number of μ evaluations required to compute the robust flutter altitudes was $n_\mu = 100$ and the computational time was $t_c = 5$ sec. A patch including fewer boxes than the number of modes contributes a block to Δ_Q with a size less than 15×15. Case c, for example, is defined by four chordwise patches along the wing tip, but the total size of Δ_Q is only 18×18 (in this case limited by the total number of boxes along the wing tip chord).

For the most simple uncertainty descriptions, the computational time is comparable to a p–k analysis (in this case, the nominal flutter altitude was computed in about 2 sec using the same altitude grid). Although still modest, the computational time increases substantially for case d (232 sec). However, the computational time for case f is only about 20% of that for case d (41 sec). It is thus very desirable to develop minimum-size uncertainty descriptions, and physical insight can be very useful for this purpose. An important part of this is to use a minimum (but still sufficient) number of normal modes in the analysis.

For the cases considered here, it was sufficient to require a tolerance $k_{\text{tol}} = 10^{-4}$ in the maximizing frequency (in the golden-section search) to compute the robust flutter boundaries with a tolerance $h_{\text{tol}} = 10$ m. In case c, a minimum number of μ evaluations was required because the nominal estimate of the peak frequency was within this tolerance. This was not true for the other cases, but it was found that if the approximation

$$\mu_{\text{peak}}(h) = \mu[k_{\text{nom}}(h)] \tag{32}$$

was used in the algorithm, the difference in the flutter boundaries was hardly visible in the graphs of Fig. 6. Although this cannot be expected in general, it suggests that the simple approximation Eq. (32) can be useful in preliminary runs. For example, cases d and f required only 21μ evaluations and took about 35 and 8 sec with this approximation, respectively. Still, the same conclusion on their similar influence on the flutter altitude could be drawn.

Conclusions

In this paper, a general LFT formulation of the μ–k method was provided. The main advantage with this formulation is that simple LFT matrix operations can be used to pose the flutter equation in a form suitable for μ-analysis. It also conforms nicely with traditional frequency-domain flutter analysis. While traditional flutter analysis aims at finding the flight conditions where a critical eigenvalue crosses the stability boundary, robust flutter analysis aims at finding the flight conditions where some uncertainty of the system makes a critical eigenvalue possible.

The close relationship between traditional and robust flutter analysis was used to formulate a simple algorithm for computation of robust flutter boundaries. The use of nominal data for estimating the peak frequency makes the algorithm quite efficient in terms of the required number of μ evaluations. In turn, the computational cost for evaluating μ depends strongly on the structure and size of the uncertainty description. This makes the development of minimum-size uncertainty descriptions very important.

The algorithm was successfully applied to compute robust flutter boundaries for an F-16 fighter. By investigating different aerodynamic uncertainty descriptions for the wing tip external stores, the flutter boundary was found to be the most sensitive to perturbations of the aerodynamic twist moment. This insight was used to derive a simplified uncertainty description that decreased the computational cost substantially without compromising the critical uncertainty mechanism. The overall result was that a 10% uncertainty in the wing tip aerodynamic modeling could reduce the predicted flutter speed by 10% in the worst case.

A significant benefit of the proposed procedure for performing robust flutter analysis is that all standard tools for structural dynamics and unsteady aerodynamics are still applicable. Only modest efforts are required to extract the needed information from the analysis, and the actual robust flutter analysis can then be implemented as a separate tool. The necessary additional modeling is modest but there is still significant work to be done to build experience on how to model uncertainties and how to validate the uncertainty modeling with flight testing and ground vibration tests.

Acknowledgments

This work was financially supported by the National Aeronautics Research Program project 541 and the Swedish Defense Material Administration under contract 278294-LB664174. Special thanks are also due to Darius Sarhaddi and coworkers at Zonatech for providing important information on accessing ZAERO internals.

References

[1] Petit, C., "Uncertainty Quantification in Aeroelasticity: Recent Results and Research Challenges," *Journal of Aircraft*, Vol. 41, No. 5, 2004, pp. 1217–1229.

[2] Lind, R., and Brenner, M., *Robust Aeroservoelastic Stability Analysis*, Springer–Verlag, London, 1999.

[3] Lind, R., "Match-Point Solutions for Robust Flutter Analysis," *Journal of Aircraft*, Vol. 39, No. 1, 2002, pp. 91–99.

[4] Borglund, D., "The μ–k Method for Robust Flutter Solutions," *Journal of Aircraft*, Vol. 41, No. 5, 2004, pp. 1209–1216.

[5] Bäck, P., and Ringertz, U. T., "Convergence of Methods for Nonlinear Eigenvalue Problems," *AIAA Journal*, Vol. 35, No. 6, 1997, pp. 1084–1087.

[6] Chen, P. C., "Damping Perturbation Method for Flutter Solution: the g-Method," *AIAA Journal*, Vol. 38, No. 9, 2000, pp. 1519–1524.

[7] Borglund, D., "Upper-Bound Flutter Speed Estimation Using the μ–k Method," *Journal of Aircraft*, Vol. 42, No. 2, 2005, pp. 555–557.

[8] Rodden, W. P., and Johnson, E. H., MSC/NASTRAN Aeroelastic Analysis User's Guide, Ver. 68, MacNeal–Schwendler, Los Angeles, CA, 1994.

[9] ZAERO Programmer's Manual, Ver. 7.1, Zona Technology, Scottsdale, AZ, 2004.

[10] Zhou, K., Doyle, J. C., and Glover, K., *Robust and Optimal Control*, Prentice Hall, Upper Saddle River, NJ, 1996, Chap. 10.

[11] Kumar, A., and Balas, G. J., "An Approach to Model Validation in the μ Framework," *Proceedings of the American Control Conference*, Baltimore, MD, 1994, pp. 3021–3026.

[12] Brenner, M., "Aeroservoelastic Model Uncertainty Bound Estimation from Flight Data," *Journal of Guidance, Control and Dynamics*, Vol. 25, No. 4, 2002, pp. 748–754.

[13] Young, P., Newlin, M., and Doyle, J., "Practical Computation of the

Mixed μ Problem," *Proceedings of the American Control Conference*, Vol. 3, Institute of Electrical and Electronics Engineers, Piscataway, NJ, 1992, pp. 2190–2194.
[14] Gill, P. E., Murray, W., and Wright, M. H., *Practical Optimization*, Academic Press, London, 1981.
[15] Chen, P. C., Sarhaddi, D., and Liu, D. D., "Limit-Cycle Oscillation Studies of a Fighter with External Stores," AIAA Paper 98-1727, 1998.
[16] ZAERO Applications Manual, Ver. 7.1, Zona Technology, Scottsdale, AZ, 2004, pp. 2-172–2-189.
[17] Balas, G. J., Doyle, J. C., Glover, K., Packard, A., and Smith, R., *μ-Analysis and Synthesis Toolbox User's Guide*, MathWorks, Natick, MA, 1996, Chap. 4.